Resubmitted to Bone

15th May 2009

Bone creep can cause progressive vertebral deformity

(revision 1)

Phillip Pollintine* MSc PhD, Jin Luo PhD, Ben Offa-Jones BSc,

Patricia Dolan PhD, Michael A. Adams PhD

Department of Anatomy, University of Bristol, Bristol, UK

*Department of Mechanical Engineering, University of Bath, Bath, U.K.

Corresponding author:

Dr Michael A. Adams,

Reader in Spine Biomechanics,

Department of Anatomy,

University of Bristol,

Southwell Street,

Bristol BS2 8EJ, U.K.

M.A.Adams@bris.ac.uk

Tel: +44 (0) 117 928 8363

Fax: +44 (0) 117 925 4794

KEY WORDS: vertebral body; deformity; creep; kyphosis; bone mineral density (BMD); mechanics.

Acknowledgements: Research funded in the U.K. by Action Medical Research.

Abstract

Introduction: Vertebral deformities in elderly people are conventionally termed "fractures", but their onset is often insidious, suggesting that time-dependent (creep) processes may also be involved. Creep has been studied in small samples of bone, but nothing is known about creep deformity of whole vertebrae, or how it might be influenced by bone mineral density (BMD). We hypothesise that sustained compressive loading can cause progressive and measurable creep deformity in elderly human vertebrae.

Methods 27 thoracolumbar "motion segments" (two vertebrae and the intervening disc and ligaments) were dissected from 20 human cadavers aged 42-91 yrs. A constant compressive force of approximately 1.0 kN was applied to each specimen for either 0.5 h or 2 h, while the anterior, middle and posterior heights of each of the 54 vertebral bodies were measured at 1 Hz using a MacReflex 2D optical tracking system. This located 6 reflective markers attached to the lateral cortex of each vertebral body, with resolution better than 10 μm. Experiments were at laboratory temperature, and polythene film was used to minimise water loss. Volumetric BMD was calculated for each vertebral body, using DXA to measure mineral content, and water-immersion for volume.

Results In the 0.5 h tests, creep deformation in the anterior, middle and posterior vertebral cortex averaged 4,331, 1,629 and 614 micro-strains respectively, where 10,000 micro-strains represents 1% loss in height. Anterior creep strains exceeded posterior ($P<0.01$) so that anterior wedging of the vertebral bodies increased, by an average 0.08^{o} (STD 0.14^{o}). Similar results were obtained after 2 h, indicating that creep rate slowed considerably with time. Less than 40% of the creep strain was recovered after 2 h. Increases in anterior wedging during the 0.5 h creep test were inversely proportional to BMD, but only in a selected sub-set of 20 specimens with average BMD < 0.15 g/cm^3 ($p=0.042$). Creep deformation caused more than 5% height loss in four vertebrae, three of which had radiographic signs of pre-existing damage.

Conclusion Sustained loading can cause progressive anterior wedge deformity in elderly human vertebrae, even in the absence of fracture.

Introduction

With increasing age, many people become shorter and develop a hunched back. Some height loss and deformity is attributable to intervertebral disc degeneration, but most of it occurs in the vertebral bodies [1]. It is customary to refer to vertebral "deformities" and to classify them as shown in **Figure 1**. "Anterior wedge" deformities are the most common [2, 3] especially in mid-thoracic and thoraco-lumbar levels, and they contribute to senile kyphosis or "dowager's hump" [4, 5]. Vertebral deformities can cause pain, disability and loss of self-esteem [6-9], in men as well as women [3, 10].

Vertebral deformities are often assumed to represent fractures, but the insidious nature of their onset in many elderly people [5], and the fact that a distinct fracture plane is not always visible on radiographs, suggests that gradual time-dependent "creep" processes may contribute. Creep is continuing deformation under constant load. Intervertebral disc creep is responsible for the diurnal variation in human stature [11] and in spinal mobility [12], and is attributable to the slow expulsion of water from the proteogylcan-rich disc matrix [13]. Disc creep is entirely recoverable when the disc is unloaded because the proteoglycans suck the water back in again [14].

The possibility of comparable vertebral creep deformation is largely unexplored. Creep deformity of animal vertebrae was reported in a recent study [15] but was mostly attributable to the cartilage endplate. Other experiments have measured time-dependent deformations in small samples of cortical [16-19] and trabecular [20-23] bone subjected to sustained or repetitive loading. The mechanism of bone creep deformation is unclear, but could involve collagen fibre slipping as observed in tendons after prolonged loading [24]. It has recently been suggested that "non-traumatic vertebral fractures may be related to long-term creep effects because the trabecular bone does not have sufficient time to recover mechanically from creep deformations accumulated by prolonged static or cyclic loading" [22]. The possibility that creep could contribute to the gradual deformation of vertebrae is supported by the curious finding that human vertebrae appear to gain height if they are unloaded for a year as a result of spinal fixation [25].

Age is likely to influence vertebral creep, not only because elderly vertebrae are weaker and less dense [26], but also because old and degenerated intervertebral discs concentrate loading on to the anterior region of the vertebral body whenever the spine is flexed [27, 28], and this is the least dense and weakest part of most elderly vertebrae [27]. This raises the fascinating possibility that vertebral creep, arising from sustained spinal loading in some stooped posture, could contribute to anterior wedge deformities (**Figure 1**) and senile kyphosis.

The purpose of the present experiment is to investigate for the first time the phenomenon of creep in whole human vertebrae. We hypothesise that creep deformity is measurable in the laboratory, and

is greater anteriorly than posteriorly so that affected vertebrae develop an anterior wedge-shaped deformity.

Materials and Methods

Cadaveric material Human thoraco-lumbar spines were removed within 72 hours of death from 20 cadavers. Death was unrelated to any condition known to affect bone metabolism, and none of the subjects had experienced prolonged bed rest prior to death. Spines were dissected into 27 "motion segments" consisting of two vertebrae and the intervening disc and ligaments, and subsequently stored at -20^{o}C. The first 9 motion segments to be tested (Group A) had an average age of 75 yrs (range 48-91 yrs). Four were male and 5 were female, and the following spinal levels were included: T8/9 (1 specimen), T9/10 (1), T12/L1 (2), L1/2 (2), L2/3 (2) and L4/5 (1). The next 18 motion segments (Group B) had an average age of 67 yrs (range 42-89 yrs). Nine were male and 9 female, and the following spinal levels were included: T7/8 (1), T9/10 (2), T10/11 (5), T11/12 (3), T12/L1 (1), L1/2 (2), L2/3 (2) and L3/4 (2). Grade of disc degeneration was assessed from macroscopic features evident at dissection after testing, using the first four points of a scale of 1-5 which emphasizes tissue integrity [29, 30]. Volumetric Bone Mineral Density (BMD) was calculated for each Group B vertebral body, after testing, using DXA to measure bone mineral, and water immersion to measure volume. (Group A vertebral bodies were used for other purposes after testing.)

Mechanical testing apparatus Each motion segment was secured in two cups of dental plaster in such a manner that compressive loading could be applied evenly to its outer surfaces but without the vertebral bodies being deeply embedded (**Figure 2**). Loading was applied by a hydraulic materials testing machine (Dartec-Zwick-Roell, England) operating in "load-control". Two low-friction rollers of variable height allowed compression to be applied to a specimen maintained at some constant angle of flexion or extension. The use of this apparatus to simulate physiologically-reasonable loading has previously been justified [31]. An initial period of compressive creep loading (300 N for 15 minutes) was applied in order to reduce post-mortem disc hydration to typical physiological levels [13]. All experiments were performed at room temperature, with polythene film wrapped around the specimen to keep its surface wet (**Figure 3**).

Creep loading Each specimen was subjected to a constant compressive load, with the load being applied initially in a linear fashion over 5 s. 'Elastic deformation' was defined as all deformation recorded during load application (3-8 s) and during the first 2 s after load application. 'Creep deformation' was measured as the continuing deformation during the following period of static loading. Group A motion segments were positioned in 2^{o} of flexion (to simulate a slightly stooped posture in life) and compressed for 2 h with an average compressive stress of 0.85 MPa (equivalent

to an average force of 1.1 kN) to simulate moderate muscle forces in standing posture [32]. They were allowed to recover for a further 2 h under a load of 100N, which was sufficient to maintain the slight flexion. Testing conditions were similar for the 18 Group B motion segments (which were tested after the Group A results had been analysed), but several details were changed in order to give added insight into the creep process. Group B specimens were positioned in 0^o of flexion, and all were compressed with 1.0 kN for 0.5 h and allowed to recover under a nominal load of 3N. The small (2^o) difference in postural angle between Groups A and B is sufficient to influence stress distributions in the discs [33, 34] and so might alter creep deformations in the adjacent vertebrae.

Measuring bone creep deformation Vertebral deformations in the sagittal plane were monitored at 1 Hz using an optical 2D MacReflex system with one camera (Qualisys Ltd., Goteborg, Sweden), which located the centres of 6 reflective markers glued to map pins inserted into the lateral cortex of each vertebral body (**Figures 2 and 3**). Two markers each defined the anterior, middle and posterior height of each vertebral body, and deformations were expressed as a proportion of vertebral height at zero load, at the start of testing. Measuring vertebral deformations only in the sagittal plane increases the accuracy of this system: previous experiments have shown that it can locate the centre of each marker with in-plane resolution better than 10 μm, and is capable of measuring very small bending movements (approximately 0.01^o) of the neural arch relative to the vertebral body [31, 35]. Data were subjected to a 30-point moving-average digital smoothing in order to reduce random noise.

Intradiscal stresses, and neural arch load-bearing. Deformations of vertebral bodies depend on what proportion of the applied compressive force they actually resist, and this in turn depends on neural arch load-bearing. In order to quantify the latter, we pulled a miniature pressure transducer through each loaded intervertebral disc, summed the measured stresses over area to obtain a force, and then subtracted this force from the 1.0 kN applied force. Neural arch load-bearing was then expressed as a % of applied load. This technique has been validated previously [36] and does not interfere with vertebral body mechanics.

Statistical analysis A repeated measures mixed ANOVA was used to detect differences in creep strains between the three different regions of the vertebral body (within subject factor) and between specimens with discs of different degrees of degeneration (between subject factor). Matched-pair t-tests were used to examine differences between creep and residual strains. Linear regression was used to examine the influence of age.

Results

Typical MacReflex measurements of vertebral deformation are presented in **Figure 4A.** These "raw" data reveal random scatter in the measured marker positions which was later reduced by

smoothing. In some specimens, close analysis of the raw data suggested paradoxical movements between individual markers which would be difficult to explain in terms of bone strain, and which could have been caused by artifacts such as bending of the marker pins under load. However, such artifacts were uncommon, and inconsistent. An example is shown by the lowest graph in **Figure 4A**, which suggests that the posterior height of the vertebral body *increased* slightly during creep loading. Six vertebrae showed an increase in height, usually in the posterior cortex. Random errors generated by the MacReflex system caused considerable scatter in the raw data (**Figure 4A**), but this was less apparent in four Group B specimens that showed very high deformations (**Figure 4B**).

Smoothed MacReflex data is shown for a typical 2 h (Group A) creep test in **Figure 5**. The three graphs show strains (deformations) of the anterior, middle and posterior regions of the vertebral body cortex. In each region there was an initial elastic deformation, followed by a gradually-increasing creep deformation. The rate of creep deformation slowed with time, but equilibrium was rarely reached in 2 h. Load removal caused an immediate increase in height, which then changed little during the following 2 h, so that a residual strain persisted after testing. Creep and elastic deformations in **Figures 4** and **5** were greatest in the anterior vertebral body, and least in the posterior vertebral body.

Results for Group A specimens are summarized in **Table 1.** Vertebral body deformations are expressed in micro-strain, where 10,000 micro-strains represents 1% loss in height. Features noted in **Figures 4** and **5** are shown to be consistent findings. Creep strains during 2 h were comparable in size to initial elastic deformations. Elastic and creep deformations were greater in the anterior vertebral body compared to the posterior ($P<0.01$). No consistent or significant differences were noted between strains in the inferior and superior vertebra in each motion segment (**Table 1**) or between thoracic and lumbar vertebrae, presumably because strains are normalised for initial size. Residual strains in the anterior, middle and posterior cortex of all 18 vertebrae were less than the respective creep strains ($P<0.05$), averaging 71%, 64% and 61% of it.

For Group B specimens, results for superior and inferior vertebrae were pooled. Four specimens that showed very high creep and elastic deformations (in combination exceeding 5% strain) were removed as outliers. Average elastic and creep deformations of these four vertebrae were 33,082 (SD 7,859) and 28,625 (SD 3,549) micro-strains, respectively. Close examination of the pre-test radiographs of these four vertebrae suggested pre-existing damage in three of them (**Figure 6**). The remaining 32 Group B results **(Table 2),** which refer to 0.5 h creep tests, show greater creep deformations in the anterior vertebral body compared to the posterior ($P<0.01$), even though these specimens were loaded in pure compression. Specimen age, and grade of disc degeneration, had no significant influence on creep or elastic strains in Group B specimens, although there was a

tendency for creep deformation of the anterior and middle regions of the vertebral body to be higher adjacent to severely degenerated discs.

Greater creep deformation anteriorly increased the anterior wedging of the vertebral bodies. In the 2 h Group A tests performed in 2^o of flexion, anterior wedging increased by an average 0.09^o (STD 0.13^o, n=18). In the 0.5 h Group B tests in pure compression, this angle increased by an average 0.08^o (STD 0.14^o, n=32).

Bone mineral density (BMD) of the 36 vertebral bodies subjected to 0.5 h creep tests averaged 0.14 (SD 0.04) g/cm^3. BMD appeared to have little influence on creep deformation ($p>0.05$) if all 32 specimens (i.e. omitting the 4 outliers) were considered, but this could have been because of stress-shielding of the vertebral body by the neural arch in some specimens [27, 36]. Calculations based on our intradiscal pressure measurements indicated that neural arch load-bearing in Group B specimens varied between 0% and 42% (mean 14%). If we consider separately those 23 vertebral bodies from specimens with neural arch load-bearing < 20%, then anterior vertebral body wedging during creep showed a tendency to increase when BMD < 0.15 g/cm^3 (**Figure 7**). This became significant ($p=0.042$) if two vertebrae with suspected damage (and neural arch load-bearing < 20%) were included. Using a power-law relationship did not improve the correlation between vertebral wedging and BMD.

When creep strains in both vertebral bodies of Group B motion segments (less the 4 outliers) were summed and compared with creep deformation in the disc (measured by the MaxReflex system from the same markers) it was found that bone contributed 24%, 11% and 3% of creep height loss by the anterior, middle and posterior regions of the motion segment, respectively. Evidently, most creep deformation occurs in the disc, but the contribution from vertebral bone is not insignificant in elderly specimens, especially anteriorly.

Discussion

Summary of findings The smooth nature of the creep deformation graphs (**Figures 4B** and **5)** indicate a slow continuous mechanism of vertebral height loss that justifies the term "creep". Creep is greatest in the anterior vertebral body, even under pure compressive loading, so that the bone develops an anterior wedging deformity. Results therefore support our hypothesis: they show that sustained compressive loading can cause progressive and measurable creep deformity in elderly human vertebrae.

Strengths and weaknesses of the study. The main strength of the present study is that it was performed on elderly human vertebrae that were loaded in a natural manner by an adjacent

intervertebral disc. Another strength is the use of a non-contact strain-measuring device with sufficient sensitivity to detect very small vertebral deformations, albeit in two dimensions.

The main weakness is that the study was performed on dead tissue, which is incapable of remodeling, and at room temperature. There is no reason to believe that death *per se* can substantially alter the mechanical properties of bone, although post-mortem blood clotting can probably hinder the flow of water through the vertebral endplate [14]. Post-mortem frozen storage has little if any effect on the known elastic properties of bone [37], but it could conceivably affect bone's time-dependent properties which are poorly understood (see below). Time-dependent visco-elastic strains increase in many materials at increasing temperature, so it might be anticipated that vertebral creep would be faster in living people (at 37^{o}C) than in the present experiments. However, these were preliminary experiments investigating a new phenomenon, and we suggest that testing at laboratory temperature is an acceptable first step, especially considering that the introduced artifact almost certainly reduced the size of the novel phenomenon investigated. Also, the fact that the rate of creep deformation slowed markedly during the testing period (**Figure 5**) suggests that creep rate is not the most important consideration: rather it is creep strain at equilibrium (if such an equilibrium exists) that would determine the extent of vertebral creep deformity in living people. Equilibrium strain may be less affected by temperature than creep rate. Creep recovery also could depend on temperature and on the presence of circulating blood, so the incomplete recovery noted in the present experiments is an unreliable guide as to what might happen in-vivo. Despite these problems, the experiment demonstrates that whole human vertebrae do creep, and indicates lower bounds for the size of the phenomenon in living people.

Relationship to other studies. No previous experiment has considered creep deformation in whole human bones, although time-dependent deformations have been studied in small pieces of cortical or trabecular bone, as described in the Introduction. The majority of these other experiments concerned tissues from young animals, and "creep" was usually equated with the residual strain following cyclic loading, which may not be entirely valid [23] because residual strains would include the effects of damage sustained at higher (peak) loads, and the effects of dynamic fatigue. Nevertheless their results are broadly compatible with those of the current study. For example, Yamamoto et al. performed creep tests for up to 35 h on small samples of trabecular bone from human vertebrae, and found that "creep" (residual) strains approached an equilibrium, when they were similar in magnitude to the initial elastic strains [22]. Creep and elastic strains were also similar to each other in the present experiment (**Tables 1** and **2**) and the rapid decrease in creep rate with time (Figure 5) suggests that creep deformation would not have increased greatly if the tests had been more prolonged.

Explanation of results Bone creep deformation is greater in the anterior region of the vertebral body because bone here has reduced BMD, and its trabecular organisation is often disrupted, so the tissue is weaker and less able to resist applied loading [27]. Small angles of flexion can concentrate compressive stress on the anterior vertebral body if the intervertebral disc is degenerated [27, 28] but this is unlikely to have had much influence because flexion was not required to create anterior wedging in the Group B specimens, which were tested in pure compression. Severe disc degeneration concentrates compressive loading on to the adjacent annulus [38] (and hence on to the adjacent vertebral cortex) and this could explain the tendency for increased bone creep deformation adjacent to grade 4 discs. It seems likely that pre-existing damage in four of the Group B specimens lead to exceptionally high creep and elastic deformations. These outliers give insights into the mechanisms of vertebral creep, which is currently being followed up. The immediate increase in specimen height when the applied load was removed (**Figure 5**) probably represents recovery of the initial elastic deformation, whereas the persisting residual strain after 2 h suggests only 30-40% recovery of creep strain.

The underlying mechanism of bone creep is not clear, but some inferences can be made from the present results. Firstly, the smoothness of the creep deformation curves (**Figures 4B** and **5**) indicates that the continuing deformation does not represent a series of minor fractures, although a long series of micro-fractures to individual trabeculae remains a possibility. Secondly, the lack of substantial creep recovery suggests that fluid flow is unlikely to be the dominant mechanism underlying bone creep (as it is in articular cartilage and intervertebral discs) because fluid flow is readily reversible when loading is removed. Thirdly, the finding that vertebral creep deformation is more rapid in the relatively weak anterior region suggests that creep is a threshold phenomenon that becomes substantial only when local tissue strength (and BMD) falls below some critical value, as suggested by **Figure 7**. This in turn raises the possibility of creep occurring as a slipping mechanism within the bone matrix once some internal resistance is overcome. Slipping could conceivably occur between adjacent bone lamellae, or at the cement lines. Creep causes the total (elastic + creep) deformation in the anterior vertebral body (**Table 2**) to exceed the elastic yield strain of trabecular bone [39], suggesting that creep may involve plastic deformation of the matrix. The present experiment actually measured strain in the vertebral cortex rather than in trabecular bone, but it is likely that both would deform in a similar manner because yield strain does not differ greatly between cortical and trabecular bone [40].

Previous experiments give additional insights into possible creep mechanisms. Compressive creep (residual deformation) of cortical bone specimens differs from tensile creep, and shows some characteristics of being a threshold phenomenon [16, 18]. Residual strains following static and

cyclic compressive loading of human trabecular bone are similar to each other, suggesting a single underlying mechanism, and full recovery of such creep deformation probably take 20 times longer than the period of loading (even at 37^{o}C) [22]. Residual strains in human cortical bone are associated with damage caused by the continuous accumulation of internal microcracks [19], especially when loading rates are slow [41]. Taking all of this evidence into account suggests that the gradual vertebral deformity observed in the present experiment (**Figure 5**) was predominantly due to microcracking of the bone matrix, which throws increased loading on to the collagenous component of the matrix which then creeps by relative gliding and rearrangement of microfibrils.

Clinical implications. Living people do adopt fixed spinal postures for 0.5 - 2 h, for example when driving, although it is more usual to apply cyclic loading to the back. In living tissues, some of the effects of bone creep can be reversed by cell-mediated remodeling processes, as observed in young rats [42]. However, elderly human bone has a greatly reduced ability to remodel microdamage [43] so that some creep deformity could accumulate over time. Despite uncertainty over the time-scale, the present experiment shows that deformity of elderly human vertebrae can not always be attributed to fracture, and that continuous creep processes at the microscopic level can contribute to deformity. Elderly people should be encouraged not to adopt stooped postures for long periods of time, because spinal flexion increases loading of the anterior region of the thoracolumbar vertebral bodies [27, 44] and could lead to anterior wedge deformity even if spinal loading remained below the levels required to cause fracture. For the same reason, vertebral deformity could possibly be minimised by wearing orthoses that inhibit spinal flexion.

Unanswered questions and future research. Currently we are investigating how creep deformation is accelerated in the presence of vertebral (micro) damage, and by body temperature. Future work should explore the molecular mechanisms of bone creep, and longitudinal studies on patients are required to assess the impact of creep in living vertebrae.

Figure Legends

Figure 1. The three common types of thoracolumbar vertebral deformity: A – anterior wedge; B – biconcave; C – crush. Reproduced with permission from Rao & Singrakhia.[45]

Figure 2. Apparatus for applying static compressive loading to cadaveric thoracolumbar motion segments. The motion segment is secured in two cups of dental plaster and the compressive load is applied by means of two low-friction rollers. The height of the rear roller could be decreased to position the specimen in 2^{o} of flexion during 2 h creep tests. Three reflective markers (black dots) indicate the superior and inferior margins of each vertebral body. Compressive loading was applied perpendicular to the mid-transverse plane of the disc.

Figure 3. Motion segment during creep loading. Three reflective markers indicate the superior and inferior margins of each vertebral body in its anterior, middle and posterior regions. Polythene film kept the surface of the specimen wet.

Figure 4. MacReflex data (unsmoothed) showing deformations of the posterior, middle and anterior vertebral body during the first 50 s. of creep tests. (A) This specimen showed typical deformations of several thousand micro-strains. Note the considerable random errors. Compressive strains are shown as positive, so the posterior vertebral body appears to increase slightly in height when loading is applied, possibly as a result of pin-movement artefact. (B) Much larger deformations occurred in four Group B vertebrae, including this one (Female, aged 52 yrs, T11/12). "Elastic" deformations were defined as those occurring during load application (3-8 s) and during the following 2 s, and "creep deformation" was defined as all deformation after 10 s. These deformations are labelled for the anterior vertebral body.

Figure 5. Creep deformation and recovery curves (after smoothing) for a typical 2 h creep test. (Male, aged 80 yrs, L2.) The three graphs show deformation (strains) in the posterior, middle and anterior vertebral body of one of the specimen's two vertebrae. Elastic (ε_{el}), creep (ε_{cr}) and residual strains (ε_{res}) are labelled for the anterior vertebral body.

Figure 6. Sagittal plane radiograph of a Group B motion segment before testing (anterior on right). Trabecular bone behind the lower endplate of the upper vertebra appears to be disturbed, suggesting pre-existing endplate damage. This was one of four vertebrae that showed combined elastic and creep deformations greater than 50,000 micro-strains (5% height loss). (Female, aged 52yrs, T11/12.)

Figure 7. Increased anterior wedging of the vertebral body during 0.5 h creep loading appeared to depend on volumetric BMD. Data is presented for all specimens in which neural arch load-bearing was less than 20%, and so would not have interfered greatly in the creep process. In vertebral

bodies with BMD <0.15 g/cm^3, anterior wedging increased as BMD decreased, but this was significant only if two specimens were included (solid symbols) which may have been damaged prior to testing (r^2=0.21, p=0.042, n=20).

References

[1] Manns RA, Haddaway MJ, McCall IW, Cassar Pullicino V, Davie MW. The relative contribution of disc and vertebral morphometry to the angle of kyphosis in asymptomatic subjects. Clin Radiol 1996;51: 258-62.

[2] Ismail AA, Cooper C, Felsenberg D, Varlow J, Kanis JA, Silman AJ, O'Neill TW. Number and type of vertebral deformities: epidemiological characteristics and relation to back pain and height loss. European Vertebral Osteoporosis Study Group. Osteoporos Int 1999;9: 206-13.

[3] Mann T, Oviatt SK, Wilson D, Nelson D, Orwoll ES. Vertebral deformity in men. J Bone Miner Res 1992;7: 1259-65.

[4] Cortet B, Houvenagel E, Puisieux F, Roches E, Garnier P, Delcambre B. Spinal curvatures and quality of life in women with vertebral fractures secondary to osteoporosis. Spine 1999;24: 1921-5.

[5] Cortet B, Roches E, Logier R, Houvenagel E, Gaydier-Souquieres G, Puisieux F, Delcambre B. Evaluation of spinal curvatures after a recent osteoporotic vertebral fracture. Joint Bone Spine 2002;69: 201-8.

[6] Burger H, Van Daele PL, Grashuis K, Hofman A, Grobbee DE, Schutte HE, Birkenhager JC, Pols HA. Vertebral deformities and functional impairment in men and women. J Bone Miner Res 1997;12: 152-7.

[7] Cockerill W, Lunt M, Silman AJ, Cooper C, Lips P, Bhalla AK, Cannata JB, Eastell R, Felsenberg D, Gennari C, Johnell O, Kanis JA, Kiss C, Masaryk P, Naves M, Poor G, Raspe H, Reid DM, Reeve J, Stepan J, Todd C, Woolf AD, O'Neill TW. Health-related quality of life and radiographic vertebral fracture. Osteoporos Int 2004;15: 113-9.

[8] Ettinger B, Black DM, Nevitt MC, Rundle AC, Cauley JA, Cummings SR, Genant HK. Contribution of vertebral deformities to chronic back pain and disability. The Study of Osteoporotic Fractures Research Group. J Bone Miner Res 1992;7: 449-56.

[9] Cockerill W, Ismail AA, Cooper C, Matthis C, Raspe H, Silman AJ, O'Neill TW. Does location of vertebral deformity within the spine influence back pain and disability? European Vertebral Osteoporosis Study (EVOS) Group. Ann Rheum Dis 2000;59: 368-71.

[10] Ismail AA, O'Neill TW, Cooper C, Silman AJ. Risk factors for vertebral deformities in men: relationship to number of vertebral deformities. European Vertebral Osteoporosis Study Group. J Bone Miner Res 2000;15: 278-83.

[11] Botsford DJ, Esses SI, Ogilvie-Harris DJ. In vivo diurnal variation in intervertebral disc volume and morphology. Spine 1994;19: 935-40.
[12] Dolan P, Adams MA. Recent advances in lumbar spinal mechanics and their significance for modelling. Clin Biomech 2001;16: S8-S16.
[13] McMillan DW, Garbutt G, Adams MA. Effect of sustained loading on the water content of intervertebral discs: implications for disc metabolism. Ann Rheum Dis 1996;55: 880-7.
[14] van der Veen AJ, van Dieen JH, Nadort A, Stam B, Smit TH. Intervertebral disc recovery after dynamic or static loading in vitro: Is there a role for the endplate? J Biomech 2007;40: 2230-5.
[15] van der Veen AJ, Mullender MG, Kingma I, van JH, Smit TH. Contribution of verftebral bodies, endplates, and intervertebral discs to the compression creep of spinal motion segments. J Biomech 2008;41: 1260-8.
[16] Fondrk M, Bahniuk E, Davy DT, Michaels C. Some viscoplastic characteristics of bovine and human cortical bone.[see comment]. J Biomech 1988;21: 623-30.
[17] Cotton JR, Zioupos P, Winwood K, Taylor M. Analysis of creep strain during tensile fatigue of cortical bone. J Biomech 2003;36: 943-9.
[18] George WT, Vashishth D. Damage mechanisms and failure modes of cortical bone under components of physiological loading. J Orthop Res 2005;23: 1047-53.
[19] Zioupos P, Wang XT, Currey JD. The accumulation of fatigue microdamage in human cortical bone of two different ages in vitro. Clin Biomech 1996;11: 365-75.
[20] Bowman SM, Keaveny TM, Gibson LJ, Hayes WC, McMahon TA. Compressive creep behavior of bovine trabecular bone. J Biomech 1994;27: 301-10.
[21] Bowman SM, Guo XE, Cheng DW, Keaveny TM, Gibson LJ, Hayes WC, McMahon TA. Creep contributes to the fatigue behavior of bovine trabecular bone. J Biomech Eng 1998;120: 647-54.
[22] Yamamoto E, Paul Crawford R, Chan DD, Keaveny TM. Development of residual strains in human vertebral trabecular bone after prolonged static and cyclic loading at low load levels. J Biomech 2006;39: 1812-8.
[23] Moore TL, O'Brien FJ, Gibson LJ. Creep does not contribute to fatigue in bovine trabecular bone. J Biomech Eng 2004;126: 321-9.
[24] Sasaki N, Shukunami N, Matsushima N, Izumi Y. Time-resolved X-ray diffraction from tendon collagen during creep using synchrotron radiation. J Biomech 1999;32: 285-92.
[25] Kermani HR, Soroush Z. Effect of long-term axial spinal unloading on vertebral body height in adult thoracolumbar spine. Eur Spine J 2008;17: 965-9.
[26] Bell GH, Dunbar O, Beck JS, Gibb A. Variations in strength of vertebrae with age and their relation to osteoporosis. Calcif Tissue Res 1967;1: 75-86.

[27] Adams MA, Pollintine P, Tobias JH, Wakley GK, Dolan P. Intervertebral disc degeneration can predispose to anterior vertebral fractures in the thoracolumbar spine. J Bone Miner Res 2006;21: 1409-16.

[28] Luo J, Skrzypiec DM, Pollintine P, Adams MA, Annesley-Williams DJ, Dolan P. Mechanical efficacy of vertebroplasty: Influence of cement type, BMD, fracture severity, and disc degeneration. Bone 2007;40: 1110-9.

[29] Adams MA, Dolan P, Hutton WC. The stages of disc degeneration as revealed by discograms. J Bone Joint Surg [Br] 1986;68: 36-41.

[30] Adams MA, Roughley PJ. What is Intervertebral Disc Degeneration, and What Causes It? Spine 2006;31: 2151-2161.

[31] Zhao F, Pollintine P, Hole BD, Dolan P, Adams MA. Discogenic origins of spinal instability. Spine 2005;30: 2621-30.

[32] Sato K, Kikuchi S, Yonezawa T. In vivo intradiscal pressure measurement in healthy individuals and in patients with ongoing back problems. Spine 1999;24: 2468-74.

[33] Adams MA, McNally DS, Chinn H, Dolan P. Posture and the compressive strength of the lumbar spine. Clin Biomech 1994;9: 5-14.

[34] Adams MA, May S, Freeman BJ, Morrison HP, Dolan P. Effects of backward bending on lumbar intervertebral discs. Relevance to physical therapy treatments for low back pain. Spine 2000;25: 431-7; discussion 438.

[35] Green TP, Allvey JC, Adams MA. Spondylolysis. Bending of the inferior articular processes of lumbar vertebrae during simulated spinal movements. Spine 1994;19: 2683-91.

[36] Pollintine P, Przybyla AS, Dolan P, Adams MA. Neural arch load-bearing in old and degenerated spines. J Biomech 2004;37: 197-204.

[37] Sedlin ED, Hirsch C. Factors affecting the determination of the physical properties of femoral cortical bone. Acta Orthop Scand 1966;37: 29-48.

[38] Adams MA, McNally DS, Dolan P. 'Stress' distributions inside intervertebral discs. The effects of age and degeneration. J Bone Joint Surg Br 1996;78: 965-72.

[39] Morgan EF, Bayraktar HH, Yeh OC, Majumdar S, Burghardt A, Keaveny TM. Contribution of inter-site variations in architecture to trabecular bone apparent yield strains. J Biomech 2004;37: 1413-20.

[40] Bayraktar HH, Morgan EF, Niebur GL, Morris GE, Wong EK, Keaveny TM. Comparison of the elastic and yield properties of human femoral trabecular and cortical bone tissue. J Biomech 2004;37: 27-35.

[41] Zioupos P, Hansen U, Currey JD. Microcracking damage and the fracture process in relation to strain rate in human cortical bone tensile failure. J Biomech 2008;41: 2932-9.

[42] Lynch JA, Silva MJ. In vivo static creep loading of the rat forelimb reduces ulnar structural properties at time-zero and induces damage-dependent woven bone formation. Bone 2008;42: 942-9.

[43] Schaffler MB, Choi K, Milgrom C. Aging and matrix microdamage accumulation in human compact bone. Bone 1995;17: 521-25.

[44] Keller TS, Harrison DE, Colloca CJ, Harrison DD, Janik TJ. Prediction of osteoporotic spinal deformity. Spine 2003;28: 455-62.

[45] Rao RD, Singrakhia MD. Painful osteoporotic vertebral fracture. Pathogenesis, evaluation, and roles of vertebroplasty and kyphoplasty in its management. J Bone Joint Surg Am 2003;85-A: 2010-22.

Table(s)

Table 1. Elastic and creep strains in the vertebral body recorded during the 2 h creep tests on 18 vertebrae (9 motion segments) in Group A. Values refer to the mean ± SD. Units are micro-strains, where 10,000 micro-strains = 1% deformation. For convenience, compressive strains are positive. *Significantly different from posterior deformations (P<0.01).

	Bone Strain (μstrain)		
UPPER vertebra (n=9)	Anterior	Middle	Posterior
Elastic deformation	1,885*±1,104	1,469±986	1,246±723
Creep deformation	3,133*±2,283	2,192±2,154	1,204±976
Residual deformation	2,540*±1,592	1,046±1,420	794±447
LOWER vertebra (n=9)			
Elastic deformation	2,018*±2,983	1,494±638	1,675±1,305
Creep deformation	2,867*±2,527	1,048±1,120	1,164±1,026
Residual deformation	1,727*±1,088	1,017±1,079	655±1140

Table 2. Elastic and creep strains in the vertebral body recorded during the 0.5 h creep tests on 32 Group B vertebrae (18 motion segments, with 4 outliers excluded). Values refer to the mean ± SD. Units are micro-strains, where 10,000 micro-strains = 1% deformation. For convenience, compressive strains are positive. *Significantly different from posterior deformations (P<0.01).

	Bone Strain (μstrain)		
	Anterior	Middle	Posterior
Elastic deformation	6,936±12,045	3,014±8,389	3,879±6,358
Creep deformation	4,331*±6,761	1,629±5,976	614±2,768
Total (elastic + creep)	11,268*±16,879	4,644±13,187	4,494±8,105

Figure 1

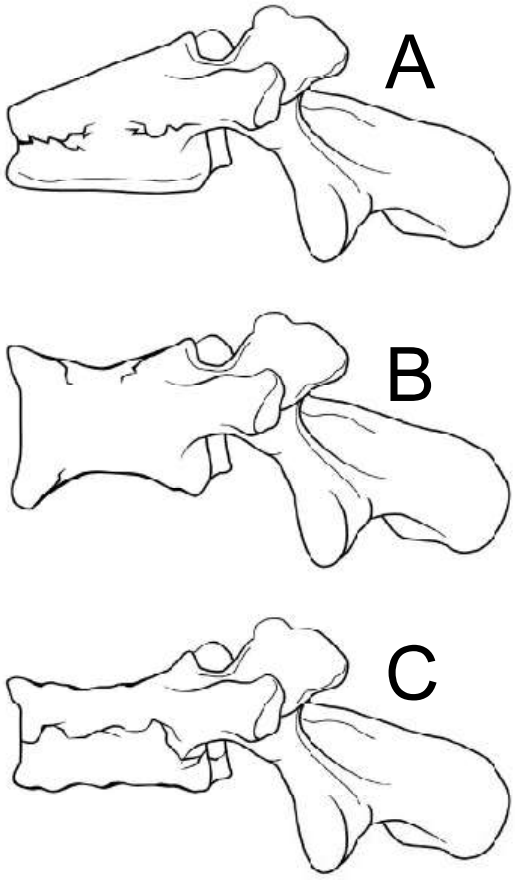

Figure 2

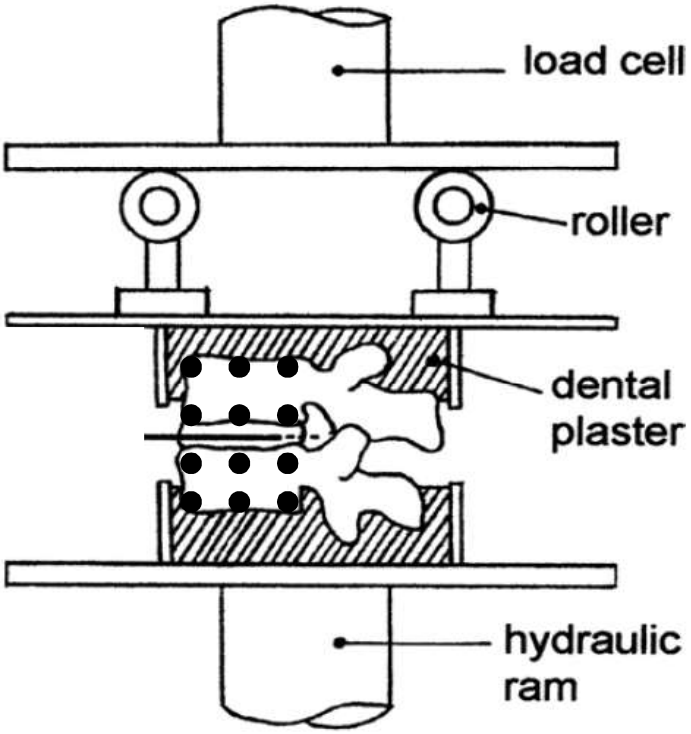

Figure 3

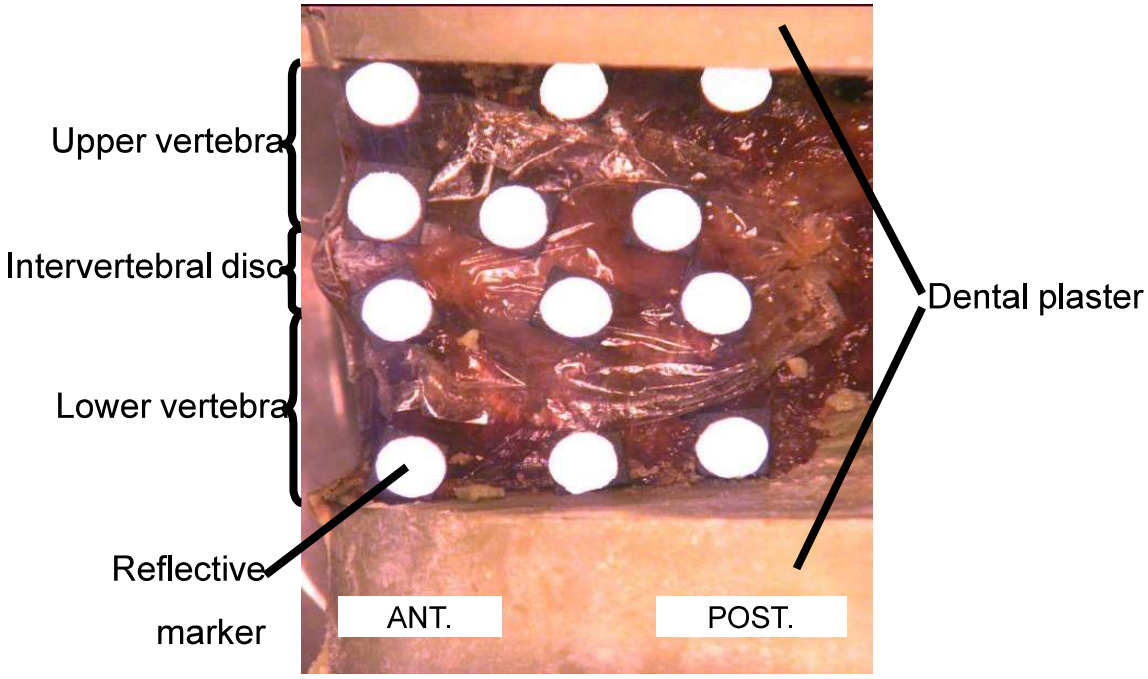
Upper vertebra
Intervertebral disc
Lower vertebra
Reflective marker
Dental plaster
ANT.
POST.

Figure 4

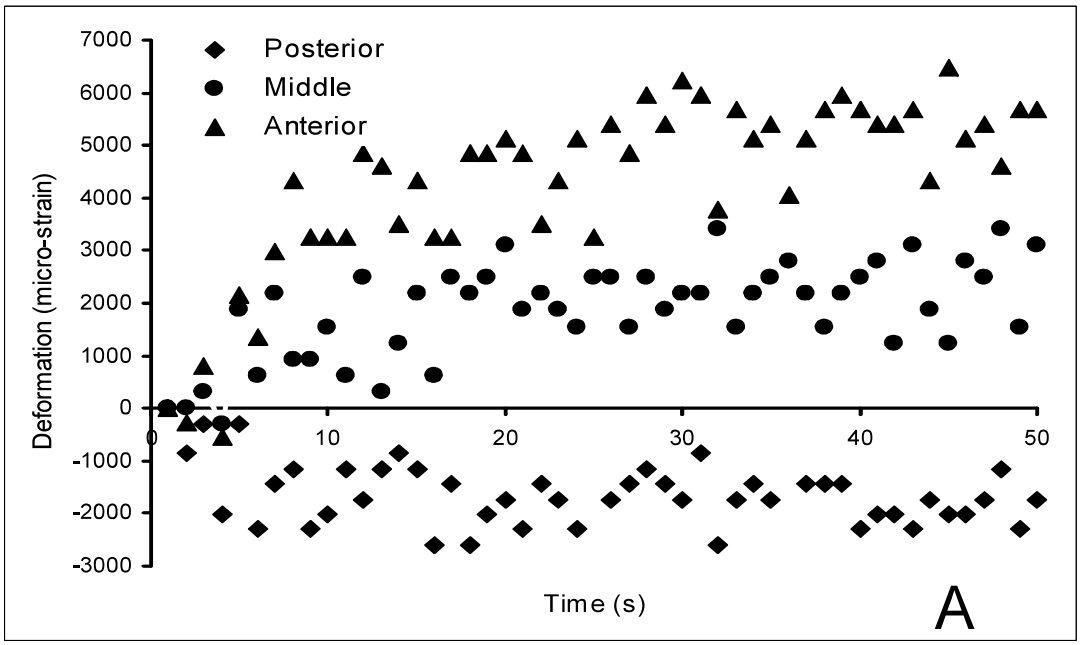
Posterior
Middle
Anterior
Deformation (micro-strain)
Time (s)
A

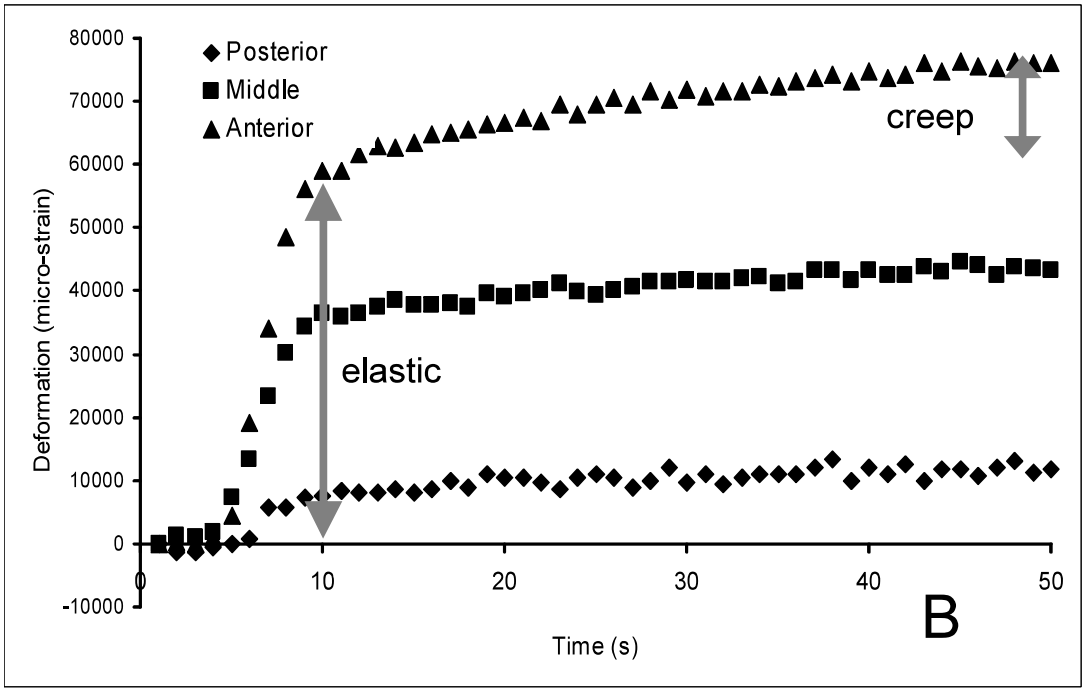
Posterior
Middle
Anterior
creep
elastic
Deformation (micro-strain)
Time (s)
B

Figure 5

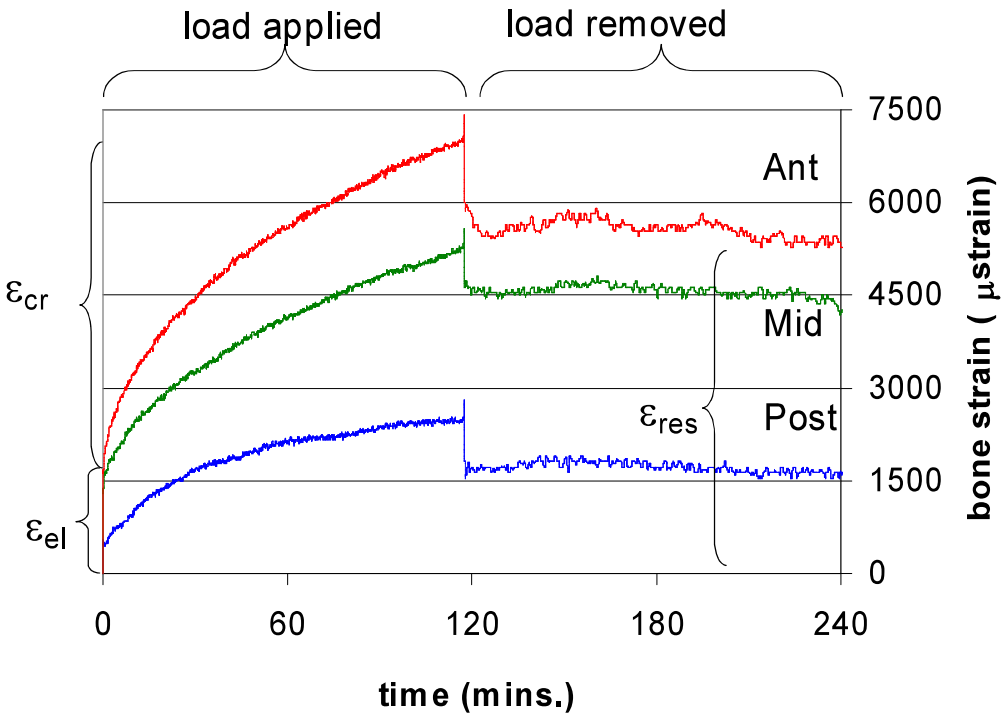

Figure 6

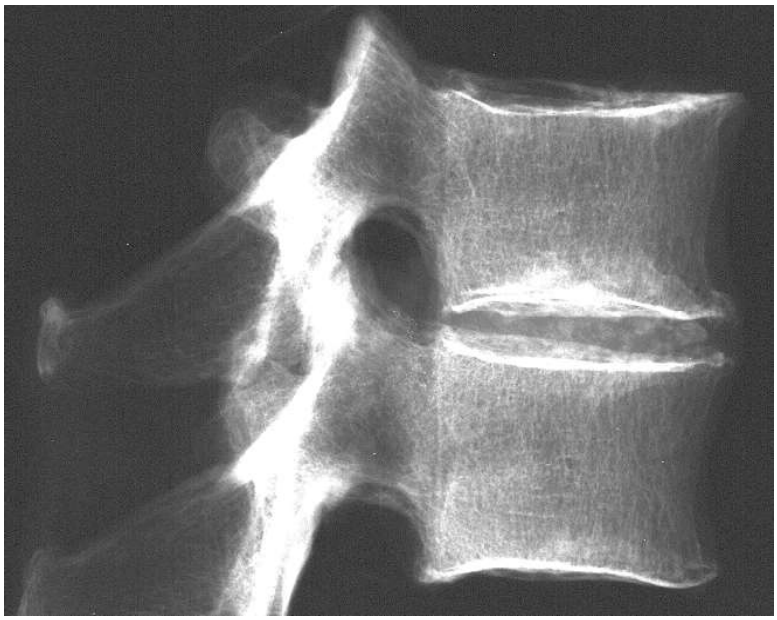

Figure 7

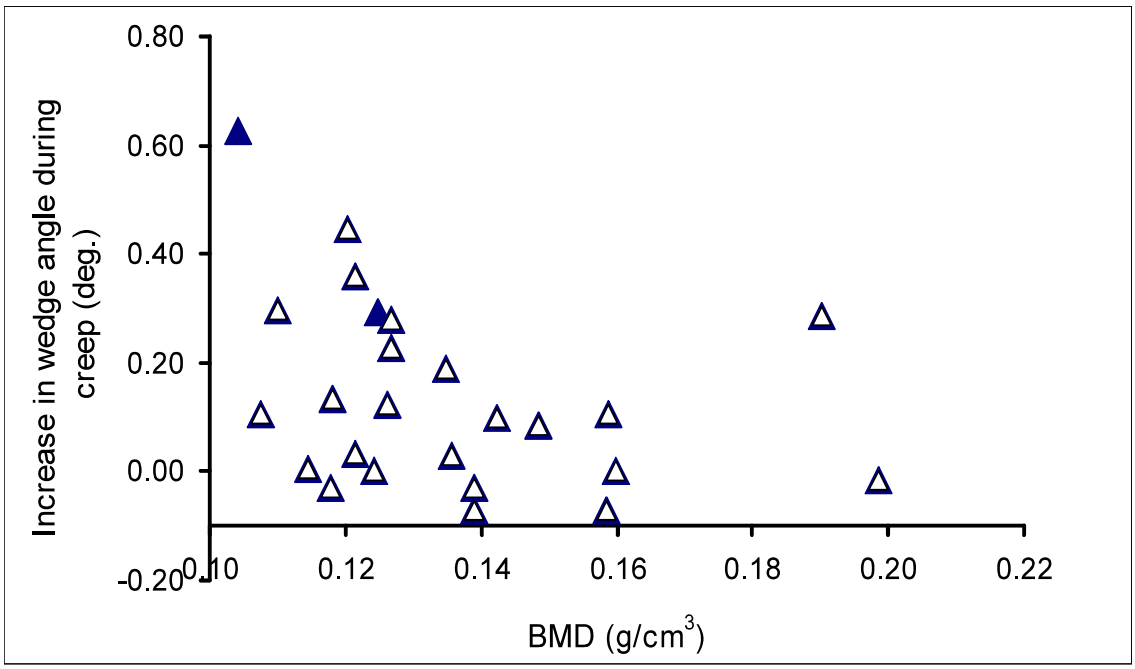
0.80
0.60
0.40
0.20
0.00
-0.20
0.10
0.12
0.14
0.16
0.18
0.20
0.22
Increase in wedge angle during creep (deg.)
BMD (g/cm3)